J|A|C|S
COMMUNICATIONS

Published on Web 09/03/2004

Aptamer-Functionalized Au Nanoparticles for the Amplified Optical Detection of Thrombin

Valeri Pavlov, Yi Xiao, Bella Shlyahovsky, and Itamar Willner*

Institute of Chemistry, The Farkas Center for Light-Induced Processes, The Hebrew University of Jerusalem, Jerusalem 91904, Israel

Received May 23, 2004; E-mail: willnea@vms.huji.ac.il

Biomaterial-metallic nanoparticle (NP) hybrid systems are extensively used in different bioanalytical applications.[1] Metallic NPs, e.g., Au or Ag NPs, coupled to biomolecules such as nucleic acids[2] or antigens (or antibodies)[3] were employed as active units in different biosensing systems.[4] Biosensing of DNA was accomplished by using metallic NPs as electrochemical markers,[5] by the application of NPs as catalytic labels for the enlargement of the NPs and the generation of conductive paths across electrodes[6] and the use of metallic NPs as labels for the amplified quartz crystal microbalance (QCM) detection of DNA.[7] Also, the optical properties of metallic NPs were employed to follow biorecognition events.[8] The selection and synthesis of aptamers is a common biochemical practice.[9] The specific aptamer−protein interactions were employed to develop label-free biosensors[10] such as the surface plasmon resonance detection of the HIV−Tat protein.[11] Also, the optical detection of aptamer−protein interactions was reported using fluorescence[12] or evanescent wave-induced fluorescence.[13] The specific interaction between thrombin and its binding aptamer has been investigated,[14] and the colorimetric detection of the aptamer−thrombin interactions was followed with polythiophene polyelectrolyte chromophores.[15] Here we report on the use of an aptamer-functionalized Au NP as a catalytic label for the amplified detection of thrombin in solution and on surfaces.

Au NPs (12 ± 1 nm) stabilized by citrate were functionalized with the thiolated aptamer, (**1**), (average loading ca. 80 aptamer units per particle). The (**1**)-functionalized Au NPs were then reacted with thrombin. Since thrombin includes two binding sites for the aptamer,[14] the thrombin-induced aggregation of the Au NPs is anticipated. The Au NPs, 6×10^{-10} M, were reacted with different concentrations of thrombin for a constant time interval of 45 min. At high concentrations of thrombin, some turbidity was observed in the solution. The resulting (**1**)-functionalized Au NP systems that include different concentrations of thrombin were centrifuged, and the absorption spectra of the solution were recorded (Figure 1A). The decrease in the plasmon absorbance is consistent with the fact that the Au NPs aggregate and precipitate from the reaction medium. Addition of the Au NP label-free aptamer (**1**) to the thrombin/(**1**) Au NPs aggregates resolubilizes the aggregates by exchanging the labeled aptamer with (**1**). Control experiments indicate that the addition of other proteins (BSA or human IgG antibodies, 200 nM) does not lead to precipitation of the (**1**)-functionalized Au NPs, implying that the precipitation originates from the specific aptamer−thrombin binding. Also, the nucleic acid (**2**)-functionalized Au NPs[16] do not bind to thrombin and do not lead to aggregation of Au NPs (**2** is not a thrombin aptamer).

The resulting precipitates formed in the different systems were then separated from the Au NP solution, and the Au NP aggregates were redissolved in an aqueous growth solution that included cetyl trimethylammonium bromide (CTAB) as surfactant. The resuspended Au NP aggregates were then used as seeds for their catalytic enlargement in the presence of $HAuCl_4$, 1.8×10^{-4} M, and NADH, 4×10^{-4} M.[17]

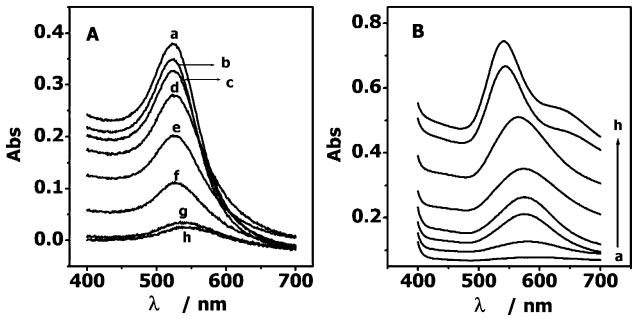

Figure 1. (A) Absorbance spectra of buffer solutions that include different concentrations of thrombin after the treatment with (**1**)-functionalized Au NPs, 6×10^{-10} M, followed by the precipitation of the generated aggregates by centrifugation. (B) Absorbance spectra of the enlarged (**1**)/thrombin aggregates formed upon the analysis of different concentrations of thrombin. The concentrations of thrombin in (A) and (B) are: (a) 0, (b) 20, (c) 44, (d) 67, (e) 89, (f) 111, (g) 122, and (h) 167 nM. (For detailed experimental conditions for the separation of thrombin−Au NP aggregates and their enlargement, see Supporting Information, p 1.)

Figure 1B shows the absorbance spectra of the enlarged CTAB-stabilized Au NP aggregates. As the concentration of thrombin in the parent solution becomes higher, the absorbance spectra after enlargement exhibit higher intensities. This is consistent with the fact that at higher thrombin concentrations the aggregate content increases, and thus more seeds are enlarged. The derived calibration curve is provided as Supporting Information p 2. The sensitivity limit for the detection of thrombin is ca. 20 nM. This value is ca. 5-fold better than the recently reported colorimetric detection of thrombin using an organic polymer chromophore. The increase in the plasmon absorbance at ca. 530 nm is attributed to the formation of more small-sized particles during the enhancement process that are further enlarged. The formation of the small-sized Au NPs is supported by the slight blue shift of the plasmon absorbance upon the enlargement of the aggregates. Interestingly, at high concentrations of thrombin, >120 nM, in the parent solution that contains the (**1**)-functionalized Au NPs, the absorbance spectra of the enlarged Au NP aggregates reveal, in addition to the localized plasmon band at $\lambda = 540$ nm, a second band at ca. $\lambda = 650$ nm. The red-shifted absorbance at $\lambda = 650$ nm may be partially attributed to the formation of ca. 2% rodlike nanoparticles (ca. 60 ± 10 nm long, 10 nm wide) upon the enlargement process (see SEM image in the Supporting Information p 3). Alternatively, the red-shifted band may originate from an interparticle coupled plasmon exciton. That is, the high concentration of Au NP-functionalized aptamer−thrombin aggregates results in sterically close, enlarged, NPs that mutually interact. The solution phase analysis of thrombin led to the optical sensing of thrombin on glass surfaces (Figure 2).

10.1021/ja046970u CCC: $27.50

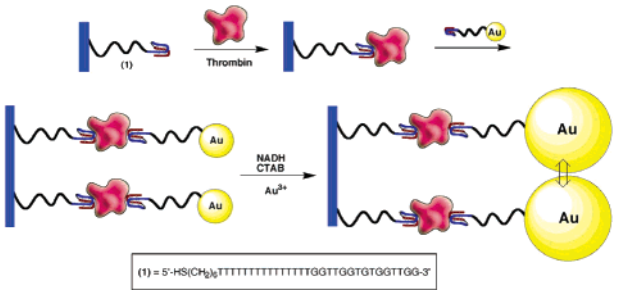

Figure 2. Amplified detection of thrombin on surfaces by the catalytic enlargement of thrombin aptamer-functionalized Au NPs.

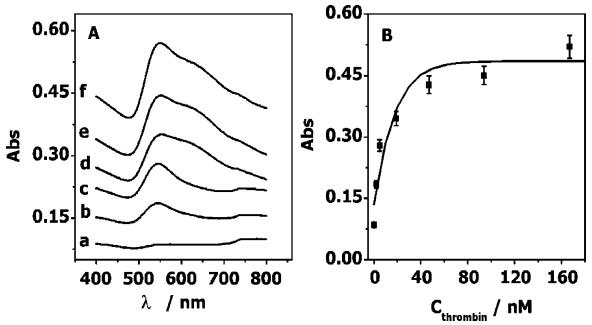

Figure 3. (A) Absorbance spectra of (**1**)-modified glass slides upon the analysis of different concentrations of thrombin using (**1**)-functionalized Au NPs and the catalytic enlargement process. Concentrations correspond to: (a) 0, (b) 2, (c) 5, (d) 19, (e) 94, and (f) 167 nM. Slides were removed from the enhancement solution and rinsed prior to the recording of the spectra. (B) Calibration curve corresponding to the amplified optical detection of thrombin.

The aptamer **1** was covalently attached to a maleimide-functionalized siloxane monolayer, and thrombin was bound to the interface. The (**1**)-functionalized Au NPs were then associated to the second thrombin binding site. The resulting Au NP interface was then enlarged in the growth solution that includes $HAuCl_4$, 1.8×10^{-4} M, CTAB, 7.4×10^{-2} M, and NADH, 4×10^{-4} M for 120 min. Figure 3A shows the absorbance spectra of functionalized surfaces upon analyzing different concentrations of thrombin. As the concentration of thrombin increases, the surface loading of bound thrombin is higher, and this results in an increased number of Au NP seeds for enlargement. As the surface density of the aptamer-functionalized Au NP is higher, the catalytic deposition of gold on the NPs is enhanced, and this is reflected by the higher absorbance spectra. At high thrombin concentrations, one observes, in addition to the plasmon band of the individual Au NP ($\lambda = 540$ nm), the coupled plasmon absorbance at $\lambda = 650$ nm.

The SEM images of the enlarged Au NPs associated with the thrombin interface reveal that as the concentration of thrombin in the sample becomes higher, the surface coverage of the enlarged particle increases. At a high thrombin concentration of 94 nM, the enlarged Au NPs are contacted, consistent with the observation of the coupled interparticle plasmon band in the optical spectrum (see Supporting Information, p 3). Figure 3B shows the resulting calibration curve.

Control experiments indicated that upon the interaction of the (**1**)-functionalized glass slides with foreign proteins (BSA or IgG Ab) no binding of the (**1**)-functionalized Au NPs to the surface occurred, and no catalytic enlargement on the surface took place. These results imply that no nonspecific adsorption of the proteins to the base aptamer or nonspecific binding of the (**1**)-functionalized Au NP to the surface occurred. The specific optical sensing of the thrombin on the surface was achieved with a sensitivity limit that corresponded to 2 nM.

The surface analysis of the aptamer−thrombin interactions by the aptamer-functionalized Au NPs was further examined using QCM measurements. The thiolated aptamer (**1**) was immobilized on Au−quartz crystals (9 MHz), resulting in a frequency change of −38 Hz that corresponds to a surface coverage of 1.0×10^{-11} mol·cm^{-2}. The interaction of the (**1**)-modified Au−quartz crystal with thrombin, 2 or 167 nM, resulted in frequency changes corresponding to −10 and −70 Hz, respectively. These values translate to surface coverage of thrombin in the systems of 6.8×10^{-13} mol·cm^{-2} and 4.8×10^{-12} mol·cm^{-2}, respectively. The subsequent association of the aptamer (**1**)-functionalized Au NPs results in a further frequency change of −30 and −240 Hz, respectively, and the catalytic enlargement of the particles leads to a decrease in the crystal frequencies that corresponds to 900 and 6000 Hz, respectively. This latter process represents an amplification path for analyzing thrombin by the aptamer-functionalized Au NPs.

Acknowledgment. This research was supported by the Nofar Program, The Ministry of Commerce, Israel.

Supporting Information Available: The calibration curve analyzing thrombin in solution, the SEM imaging of the enlarged Au NPs associated with the thrombin interfaces, and the experimental conditions for the synthesis and characterization of the Au NPs. This material is available free of charge via the Internet at http://pubs.acs.org.

References

(1) (a) Niemeyer, C. M. *Angew. Chem., Int. Ed.* **2001**, *40*, 4128−4158. (b) Katz, E.; Willner, I.; Wang, J. *Electroanalysis* **2004**, *16*, 19−44.
(2) (a) Alivisatos, A. P.; Johnsson, K. P.; Peng, X.; Wilson, T. E.; Loweth, C. J.; Bruchez M. P.; Schultz, P. G. *Nature* **1996**, *382*, 609−611.
(3) Niemeyer, C. M.; Ceyhan, B. *Angew. Chem.* **2001**, *113*, 3798−3801.
(4) He, L.; Musick, M. D.; Nicewarner S. R.; Salinas F. G.; Benkovic S. J.; Natan M. J.; Keating, C. D. *J. Am. Chem. Soc.* **2000**, *122*, 9071−9077.
(5) Wang, J.; Xu, D.; Kawde, A. N.; Polsky, R. *Anal. Chem.* **2001**, *73*, 5576−5581.
(6) Park, S. J.; Taton, T. A.; Mirkin, C. A. *Science* **2002**, *295*, 1503−1506.
(7) Weizmann, Y.; Patolsky, F.; Willner, I. *Analyst* **2001**, *126*, 1502−1504.
(8) (a) Storhoff, J. J.; Mirkin, C. A. *Chem. Rev.* **1999**, *99*, 1849−1862. (b) Elghanian, R.; Storhoff, J. J.; Mucic, R. C.; Letsinger, R. L.; Mirkin, C. A. *Science* **1997**, *277*, 1078−1081.
(9) Luzi, E.; Minunni, M.; Tombelli, S.; Mascini, M. *Trends Anal. Chem.* **2003**, *11*, 810−818.
(10) Fukusho, S.; Furusawa, H.; Okahata, Y. *Chem. Commun.* **2002**, 88−89.
(11) Kawakami, J.; Hirofumi, I.; Yukie, Y.; Sugimoto, N. *J. Inorg. Biochem.* **2000**, *82*, 197−206.
(12) Kleinjung, F.; Klussman, S.; Erdmann, V. A.; Scheller, F. W.; Furste, J. P.; Bier, F. F. *Anal. Chem.* **1998**, *70*, 328−331.
(13) Potyrailo, R. A.; Conrad, R. C.; Ellington, A. D.; Hieftje, G. M. *Anal. Chem.* **1998**, *70*, 3419−3425.
(14) (a) Bock, L. C.; Griffin, L. C.; Latham, J. A.; Vermaas, E. H.; Toole, J. J. *Nature* **1992**, *355*, 564−566. (b) Macaya, R. F.; Waldron, J. A.; Beutel, B. A.; Gao, H. T.; Joesten, M. E.; Yang, M. H.; Patel, R.; Bertelsen, A. H.; Cook, A. F. *Biochemistry* **1995**, *34*, 4478−4492. (c) Padmanabhan K.; Tulinsky A. *Acta Crystallogr.* **1996**, *D52*, 272−282.
(15) Ho, H. A.; Leclerc, M. *J. Am. Chem. Soc.* **2004**, *126*, 1384−1387.
(16) The sequence of (**2**) is: 5′HS(CH$_2$)$_6$CCCCCACGTTGTAAAACGACGG CCAGT3′.
(17) For the detailed analysis of the growth of the Au NPs in the presence of NADH/CTAB, see Xiao, Y.; Pavlov, V.; Levine, S.; Niazov, T.; Markovitch, G.; Willner, I. *Angew. Chem., Int. Ed.* **2004**, *43*, 4519−4522.

JA046970U